

Relating Electric Vehicle Charging to Speed Scaling with Job-Specific Speed Limits

Leoni Winschermann, Antonios Antoniadis, Marco E. T. Gerards, Gerwin Hoogsteen, Johann Hurink

Department of Electrical Engineering, Mathematics and Computer Science

University of Twente

Enschede, The Netherlands

{l.winschermann, a.antoniadis, m.e.t.gerards, g.hoogsteen, j.l.hurink}@utwente.nl

Abstract—Due to the ongoing electrification of transport in combination with limited power grid capacities, efficient ways to schedule the charging of electric vehicles (EVs) are needed for the operation of, for example, large parking lots. Common approaches such as model predictive control repeatedly solve a corresponding offline problem.

In this work, we first present and analyze the Flow-based Offline Charging Scheduler (FOCS), an offline algorithm to derive an optimal EV charging schedule for a fleet of EVs that minimizes an increasing, convex and differentiable function of the corresponding aggregated power profile. To this end, we relate EV charging to processor speed scaling models with job-specific speed limits. We prove our algorithm to be optimal and derive necessary and sufficient conditions for any EV charging profile to be optimal.

Furthermore, we discuss two online algorithms and their competitive ratios for a specific class objective functions. In particular, we show that if those algorithms are applied and adapted to the presented EV scheduling problem, the competitive ratios for Average Rate and Optimal Available match those of the classical speed scaling problem. Finally, we present numerical results using real-world EV charging data to put the theoretical competitive ratios into a practical perspective.

Index Terms—electric vehicle, scheduling, speed scaling

I. INTRODUCTION

Due to the on-going electrification of transport in combination with limited power grid capacities [1] and synchronization effects [2], efficient ways to schedule the charging of electric vehicles (EVs) are needed for the operation of, for example, large parking lots. In practice, however, individual vehicles come with uncertainty in their availability and energy demand [3]. To bridge this information gap, model predictive control (MPC) can be applied [4]. Such MPC frameworks introduce a (predictive) model to the scheduler that based on all information available at the current moment in time derives a control action for the next time step. Basic examples for such models are predictions based on historical data (e.g., [5]), or the introduction of deterministic charging guarantees of the form that everyone receives x units of energy within y hours (e.g., [6]). Another possible model is centered around the prediction of fill-levels that dictate the targeted aggregated power profile [7]. The resulting planning may either be updated periodically, for example every 15 minutes, or rescheduling may occur based on events, for example the arrival or (early)

departure of an EV. As a result, MPCs repeatedly solve an offline problem. This problem is characterized by the EVs' arrival times, departure times, energy demand and EV-specific maximum charging rates. EVs can charge simultaneously and charging of a single EV may be preempted.

To account for the limited grid capacity and a quadratic relation between charging powers and energy losses, one natural objective in EV scheduling problems is to minimize the sum of squares of the aggregated power profile of for example a parking lot hosting multiple EVs. EV scheduling problems with this objective naturally reduce to (processor) speed scaling problems with job-specific speed limits. Hereby, as opposed to the classical model, multiple jobs may run simultaneously. In speed scaling, tasks are scheduled on a processor within their respective availability such that a (typically increasing, convex and differentiable) function of the processing speed is minimized. One such function may correspond to the ℓ_2 -norm, a well-studied objective function in both processor scheduling and energy research. Speed scaling problems without speed limits are well-studied, with the YDS algorithm being one of the core approaches [8]. Already before YDS, [9] studied the same problem and came up with a similar solution as early as 1981. An extension of YDS considering continuous speed limits for the aggregated speed profile is given by [10]. Another variant considers job-specific speed functions and uses a maximum flow formulation to find an optimal solution for both a single-processor and multi-processor setup [11]. [12] investigate a model where changes in global speed are associated with additional cost. However, to the best of our knowledge, the use case with job-specific speed limits, as is relevant to EV scheduling with EV-specific maximum charging powers, has not yet been studied. Here, job-specific speed limits correspond to the maximum charging powers of the individual EVs.

In this work, we make the following contributions to both the understanding of the offline and online versions of the EV scheduling problem sketched above.

- We discuss the relation between the classical speed scaling model and the extension based on EV scheduling.
- We present and analyze a novel offline algorithm to derive an optimal charging schedule for a fleet of EVs, minimizing an increasing, convex and differentiable function of the aggregated speed profile.

- We derive necessary and sufficient conditions for solutions to the offline problem to be optimal.
- We derive competitive ratios for two natural algorithms for the online problem known from speed scaling without job-specific speed limits. In particular, we show average rate scheduling to be directly applicable to the extended model and to have a competitive ratio of $2^{\alpha-1}\alpha^\alpha$ for a given α -dependent objective function. The second algorithm considered is an adapted version of Optimal Available as previously studied for speed scaling without job-specific speed limits. We show it to be α^α competitive for the same objective function. Both competitive ratios match those for the corresponding algorithms applied to speed scaling without job-specific speed limits.
- We put those theoretical results in perspective using real-world data to empirically quantify the performance of average rate and Optimal Available for an EV scheduling case.
- We prove that given the aggregated speed profile of a feasible solution, there exists no deterministic online scheduling rule that reliably finds a feasible solution following the given profile.

The remainder of the paper is organized as follows. Section II formally describes the extended speed scaling model. After that, in Section III we analyze the offline problem and present the *Flow-based Offline Charging Scheduler* (FOCS), which is an offline algorithm that uses maximum flows to compute an optimal solution for the given problem. Then, Section IV extends the problem to online scheduling, considering the competitive ratios of two natural algorithms. Furthermore, we prove the non-existence of exact deterministic online scheduling rules for fill-level scheduling with more than one job. Finally, we compare theoretical competitive ratios to empirical results in Section V using numerical experiments based on real-world EV charging data. Section VI presents the conclusion of the paper.

II. PROBLEM STATEMENT

In this section, we describe the considered speed scaling models for processor scheduling with and without job-specific speed limits. Note that the used notation follows scheduling convention to emphasize the relation to classical results. In sentences that discuss energy, we caution the reader to carefully consider the context since the term refers to two related but different concepts in respectively processor scheduling and EV research.

The *Deadline-Based Speed-Scaling with Speed Limits* (DSL) problem is defined as follows. Consider a set $\mathcal{J} := \{1, \dots, n\}$ of jobs that have to be scheduled on a speed-scalable processor. Each job $j \in \mathcal{J}$ is characterized by its *workload* $p_j \in \mathbb{R}_{\geq 0}$, *release time* $r_j \in \mathbb{R}_{\geq 0}$, *deadline* $d_j \geq r_j$ as well as a *job-specific speed limit* $\ell_j \in \mathbb{R}_{\geq 0}$. A *schedule* is given by a function $s : \mathbb{R}_{\geq 0} \rightarrow (\mathbb{R}_{\geq 0})^n$, such that $s(t)$ is a vector describing at what speed each job is processed at time t . Let $s_j(t)$ be the j^{th} entry of that vector.

Definition 1: A schedule for a given set of jobs \mathcal{J} is said to be *feasible for DSL* if

- (i) every job $j \in \mathcal{J}$ is fully processed within $[r_j, d_j)$, i.e., $\int_{r_j}^{d_j} s_j(t) dt \geq p_j$,
- (ii) $s_j(t) = 0$ for $t \notin [r_j, d_j)$, and
- (iii) each job respects its speed limit, i.e., $s_j(t) \leq \ell_j$ for all $t \in \mathbb{R}_{\geq 0}$.

Note that jobs may be preempted and (in contrast to the classical speed scaling model) run simultaneously.

Definition 2: For a schedule s let $\text{PF}_s : \mathbb{R}_{\geq 0} \rightarrow \mathbb{R}_{\geq 0}$ be the *speed profile* of s defined by $\text{PF}_s(t) = \sum_j s_j(t)$.

For any schedule s , we consider a separable objective function

$$F(\text{PF}_s(t)) \quad (1)$$

of the aggregated speed profile which has to be minimized and where F is (i) convex, (ii) differentiable and (iii) has the property that strictly increasing any s_j such that value $\int_{t_i}^{t_{i+1}} s_j(t) dt$ increases for some $t_{i+1} - t_i > \epsilon > 0$ results in an increase of objective function F . For convenience, we call a function F that satisfies the property (iii) *increasing*. Note that in power applications, energy losses are quadratically correlated with the speed profile, and for dynamic voltage and frequency scaling that relation is cubic. Therefore, a natural choice for objective function F is the *energy consumption* of a schedule, given by

$$E(s) = \int_0^\infty (\text{PF}_s(t))^\alpha dt, \quad (2)$$

where $\alpha > 1$ is a constant.

In the following we assume that all considered DSL instances are *feasible*, i.e., they satisfy

$$p_j \leq \ell_j (d_j - r_j) \quad \forall j \in \mathcal{J}. \quad (3)$$

DSL is closely related to the *Deadline-Based Speed-Scaling* (DS) problem. The only difference is that inputs to DS omit the speed limits, and at most one job can run at any given time. More formally, the following conditions apply to a feasible DS schedule.

Definition 3: A schedule is said to be *feasible for DS* if

- (i) every job $j \in \mathcal{J}$ is fully processed within $[r_j, d_j)$, i.e., $\int_{r_j}^{d_j} s_j(t) dt \geq p_j$,
- (ii) $s_j(t) = 0$ for $t \notin [r_j, d_j)$, and
- (iii) at most one job runs at any time, i.e., $|\{j | s_j(t) > 0\}| \leq 1$ for all $t \in \mathbb{R}_{\geq 0}$.

The rest of the problem definition carries over from that of DSL.

III. OFFLINE SCHEDULING

As mentioned above for the MPC context, in the operational reality of EV charging DSL may be solved repeatedly. Therefore, in this section, we analyze the offline DSL problem. In particular, we analyze the relation between feasible schedules for DSL and DS (Section III-A), derive necessary and sufficient optimality conditions for offline algorithms (Section III-B), and introduce and analyze the *Flow-based Offline Charging Scheduler* (FOCS), an offline algorithm that solves DSL to optimality (Sections III-C and III-D).

A. Preliminaries offline algorithms

Let T be the set of all time points that are either a release time or a deadline of a given problem instance. Formally, $T := \{t \mid \exists j \in \mathcal{J} : t = r_j \text{ or } t = d_j\}$. We refer to the elements of T as breakpoints. Let $t_1 < t_2 < \dots < t_{m+1}$ be the sorted elements of T , whereby $1 \leq m \leq 2n - 1$, and intervals $\{[t_i, t_{i+1}) \mid i = 1, \dots, m\}$ partition the time between the earliest release time and latest deadline into subintervals. We refer to those subintervals as *atomic intervals*, and denote atomic interval $[t_i, t_{i+1})$ as M_i . Hereby, the length $t_{i+1} - t_i$ of interval M_i is denoted as $|M_i|$. Furthermore, we introduce an operator L for the combined length of a set of atomic intervals, i.e., if \mathcal{T} is a set of indices, then $L(\mathcal{T}) = \sum_{i \in \mathcal{T}} |M_i|$. We denote the set of all indices corresponding to atomic intervals by $\mathcal{M} = \{1, \dots, m\}$.

Given that the close relationship between DSL and DS plays a central role in our results it is useful to derive notation for the inputs, outputs and algorithms for each problem:

Definition 4: Let \mathcal{I}_{DSL} (resp. \mathcal{I}_{DS}) be the set of all possible inputs to DSL (resp. DS), with $I \in \mathcal{I}_{\text{DSL}}$ being described as $I = \langle \vec{r}, \vec{d}, \vec{p}, \vec{\ell} \rangle$ (resp. $I \in \mathcal{I}_{\text{DS}}$, with $I = \langle \vec{r}, \vec{d}, \vec{p} \rangle$) where $\vec{r}, \vec{d}, \vec{p}$ and $\vec{\ell}$ refer to a vector of the respective release times, deadlines, processing volume and (if applicable) speed limits describing the job set \mathcal{J} . We say that an instance $I = \langle \vec{r}, \vec{d}, \vec{p}, \vec{\ell} \rangle \in \mathcal{I}_{\text{DSL}}$ *augments* an instance $I' = \langle \vec{r}', \vec{d}', \vec{p}' \rangle \in \mathcal{I}_{\text{DS}}$ if and only if $\vec{r} = \vec{r}'$, $\vec{d} = \vec{d}'$ and $\vec{p} = \vec{p}'$. We express this as $a(I) = I'$ and call I and I' *corresponding*. Note that function $a : \mathcal{I}_{\text{DSL}} \rightarrow \mathcal{I}_{\text{DS}}$ is *not* one-to-one.

We note that a feasible schedule for an input $I' \in \mathcal{I}_{\text{DS}}$ is also feasible for input $I = a(I') \in \mathcal{I}_{\text{DSL}}$ if and only if it satisfies all job-specific speed limits.

Lemma 1: Any feasible schedule s for an instance $I = \langle \vec{r}, \vec{d}, \vec{p}, \vec{\ell} \rangle \in \mathcal{I}_{\text{DSL}}$ of the DSL problem, can be transformed into a feasible schedule s' for the corresponding augmented instance $I' = a(I) \in \mathcal{I}_{\text{DS}}$, such that both schedules have the same speed profile (i.e., $\text{PF}_s = \text{PF}_{s'}$ and therefore also $E(s) = E(s')$).

Proof of Lemma 1: Consider a schedule s that is feasible for instance $I = \langle \vec{r}, \vec{d}, \vec{p}, \vec{\ell} \rangle \in \mathcal{I}_{\text{DSL}}$, with associated job set \mathcal{J} . We show how to transform s into a schedule s' such that $\text{PF}_s = \text{PF}_{s'}$ and s' is feasible for the corresponding augmented instance $I' = a(I)$. To this end, we consider atomic intervals $M_i = [t_i, t_{i+1}) \in \mathcal{M}$ separately.

Schedule s' is obtained by simply scheduling within each interval M_i and for each job $j \in \mathcal{J}$ an amount of processing volume equal to $\int_{t_i}^{t_{i+1}} s_j(t) dt$. All these volumes are scheduled within M_i according to Earliest Deadline First (EDF) and with the same speed profile PF_s .

By the definition of s' it is straightforward that $\text{PF}_s = \text{PF}_{s'}$ and therefore it remains to argue that s' is a feasible schedule for I' . Indeed, properties (i) and (ii) as defined in Definition 3 hold because for any atomic interval M_i it is the case that $\int_{t_i}^{t_{i+1}} s_j(t) dt = \int_{t_i}^{t_{i+1}} s'_j(t) dt$ and furthermore by definition the interior of M_i contains no release time or deadline. Property (iii) follows directly by the definition of EDF. ■

Figure 1 illustrates the method applied in the proof for instances $I = \langle (0, 0), (1, 2), (1, 2), (2, 2) \rangle$ and $I' = a(I) = \langle (0, 0), (1, 2), (1, 2) \rangle$. Here, breakpoints t_0 , t_1 , and t_2 are indicated with green dashed lines.

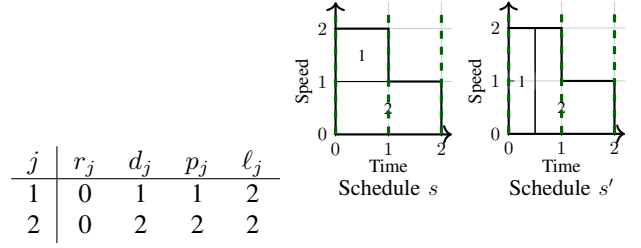


Fig. 1: Illustration of transformation applied in proof of Lemma 1.

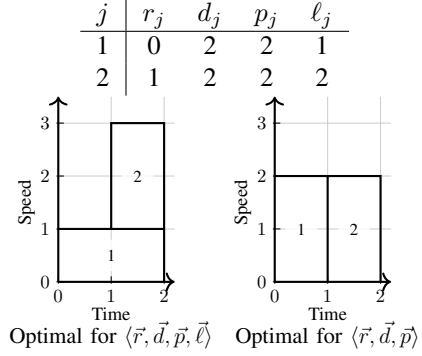


Fig. 2: Example of an instance where the optimal speed profile for DSL instance I differs from the optimal speed profile of the augmented DS instance $a(I)$ under objective function (2) with $\alpha = 2$.

Figure 2 gives an example showing that the converse statement to that of Lemma 1 is not true. It shows an instance $I = \langle \vec{r}, \vec{d}, \vec{p}, \vec{\ell} \rangle$, the corresponding instance $a(I)$, and a feasible schedule s' for DS instance $a(I)$, for which no feasible schedule for I with the exact same speed profile $\text{PF}_{s'}$ exists. Moreover, even if given a speed profile PF_s corresponding to a feasible schedule s , EDF does not necessarily result in a feasible schedule, even if it respects job-specific maximum speeds. See Figure 3 for an example of this phenomenon.

The above lemma implies the following corollary.

Corollary 1: An optimal schedule s for $I = \langle \vec{r}, \vec{d}, \vec{p}, \vec{\ell} \rangle$ consumes at least as much energy as an optimal schedule s' for $a(I) = \langle \vec{r}, \vec{d}, \vec{p} \rangle$, i.e., $E(s) \geq E(s')$.

B. Optimality conditions

In this section, we give a convex programming formulation for the considered offline EV scheduling problem to derive

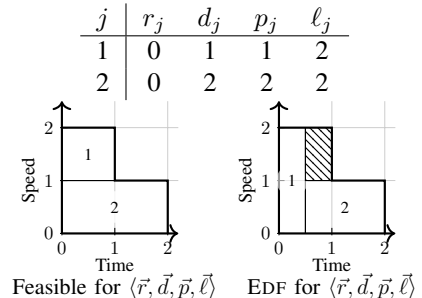


Fig. 3: Example of an instance where EDF results in an infeasible schedule for a DSL instance even when respecting speed limits.

necessary and sufficient optimality conditions. To this end, we extend the mathematical program given in [13].

First, we introduce some additional notation for the offline model. For a given atomic interval M_i , we denote by $J(i)$ the jobs that are available in interval M_i , i.e.,

$$J(i) = \{j \in \mathcal{J} | (r_j \leq t_i) \wedge (t_{i+1} \leq d_j)\}.$$

Similarly, for a job $j \in \mathcal{J}$ we define by $J^{-1}(j)$ the set of indices i for which job j is available in interval M_i . Finally, as atomic intervals are in general not unit-sized, we introduce maximum work limits $p_{i,j}^{\max} = l_j |M_i|$ per job j and interval M_i .

As decision variables, let $p_{i,j}$ be the work scheduled for job j during atomic interval M_i , i.e., $p_{i,j} = \int_{t_i}^{t_{i+1}} s_j(t) dt$ where schedule s is yet to be determined. Given those $p_{i,j}$ values, a schedule s follows naturally by scheduling job j at speed $\frac{p_{i,j}}{|M_i|}$ throughout M_i . Therefore, decision variables $p_{i,j}$ naturally correspond to a discretized EV charging schedule where all $s_j(t)$ are *step functions*, i.e., the speed between two breakpoints is constant. Moreover, note that by Jensen's inequality [14]

$$F \left(\frac{\int_{t_i}^{t_{i+1}} \text{PF}_s(t) dt}{|M_i|} \right) |M_i| \leq \int_{t_i}^{t_{i+1}} F(\text{PF}_s(t)) dt$$

for any schedule s and atomic interval M_i . Furthermore, by convexity of F , the optimal speed profile of an instant is unique. Combined, this implies that the optimal speed profile is constant within atomic intervals. As we do not consider vehicle-to-grid applications in this work, we require that $p_{i,j} \geq 0$. Together with the feasibility conditions for DSL introduced in Section II, we summarize the mathematical model for DSL as follows:

$$\sum_{i \in J^{-1}(j)} p_{i,j} \geq p_j \quad \forall j \in \mathcal{J} \quad (4a)$$

$$p_{i,j} \geq 0 \quad \forall j \in \mathcal{J}, i \in J^{-1}(j) \quad (4b)$$

$$p_{i,j} \leq p_{i,j}^{\max} \quad \forall j \in \mathcal{J}, i \in J^{-1}(j). \quad (4c)$$

Note that these constraints are the same as those used by [13] (up to notation), extended by Inequality (4c), which models the job-specific speed limits.

From a grid perspective, the aggregated power level resulting from an EV schedule is of interest. For a given schedule, the average aggregated speed in atomic interval M_i is given by $\frac{\sum_{j \in J(i)} p_{i,j}}{|M_i|}$.

Next, we consider the KKT conditions corresponding to the problem. Generally, for a convex program

$$\begin{aligned} \min \quad & \phi(x) \\ \text{s.t.} \quad & \psi_k(x) \leq 0 \quad k = 1, \dots, N \end{aligned}$$

with differentiable functions ψ_k are expressed using the KKT multipliers λ_k associated with ψ_k . These necessary and

sufficient conditions for optimality of solutions x and λ [15] are

$$\psi_k(x) \leq 0 \quad k = 1, \dots, N \quad (5a)$$

$$\lambda_k \geq 0 \quad k = 1, \dots, N \quad (5b)$$

$$\lambda_k \psi_k(x) = 0 \quad k = 1, \dots, N \quad (5c)$$

$$\nabla \phi(x) + \sum_{k=1}^N \lambda_k \nabla \psi_k(x) = 0. \quad (5d)$$

In this section, we consider the general form F of the objective function as defined in (1). Applying (5) to the discretized formulation of DSL (4), and introducing dual variables denoted by δ_j for (4a), $\gamma_{i,j}$ for (4b), and $\zeta_{i,j}$ for (4c), KKT condition (5d) leads to

$$\begin{aligned} 0 = \nabla F \left(\sum_{j \in \mathcal{J}} s_j(t) \right) & \\ + \sum_{j=1}^n \delta_j \nabla \left(p_j - \sum_{i \in J^{-1}(j)} p_{i,j} \right) & \\ - \sum_{i \in \mathcal{M}} \sum_{j \in J(i)} \gamma_{i,j} \nabla p_{i,j} & \\ - \sum_{i \in \mathcal{M}} \sum_{j \in J(i)} \zeta_{i,j} \nabla (p_{i,j}^{\max} - p_{i,j}). & \end{aligned}$$

Note that the component of this gradient that corresponds to the partial derivative with respect to $p_{i,j}$ is

$$0 = \frac{\partial F}{\partial p_{i,j}} - \delta_j - \gamma_{i,j} + \zeta_{i,j}. \quad (6)$$

We analyze condition (6) for components corresponding to partial derivatives with respect to $p_{i,j}$, where job $j \in J(i)$. We consider three cases in our analysis.

First, consider $0 < p_{i,j} < p_{i,j}^{\max}$. In this case job j charges in interval i , but not at full power. Complementary slackness (see (5c)), now implies that $p_{i,j} \gamma_{i,j} = 0$ and $(p_{i,j} - p_{i,j}^{\max}) \zeta_{i,j} = 0$. In the considered case, this implies that $\gamma_{i,j} = \zeta_{i,j} = 0$. Therefore, (6) simplifies to

$$\begin{aligned} 0 = -\delta_j + \frac{\partial F}{\partial p_{i,j}} & \\ \iff \delta_j = \frac{\partial F}{\partial p_{i,j}}. & \end{aligned} \quad (7)$$

This shows that the dual variable δ_j is the derivative of the intensity function F with respect to $p_{i,j}$. Since δ_j does not depend on i and F is convex and increasing, the aggregated speed needs to be the same for any atomic interval with index i' where job j charges at a rate strictly between 0 and its power limit.

Next, consider the case where $0 = p_{i,j} < p_{i,j}^{\max}$. Complementary slackness gives $\zeta_{i,j} = 0$, leaving us with

$$\begin{aligned} 0 = -\delta_j + \frac{\partial F}{\partial p_{i,j}} - \gamma_{i,j} & \\ \iff \gamma_{i,j} = -\delta_j + \frac{\partial F}{\partial p_{i,j}}. & \end{aligned} \quad (8)$$

Using non-negativity of $\gamma_{i,j}$ (see (5b)), it follows that $\frac{\partial F}{\partial p_{i,j}} \geq \delta_j$. As above, δ_j is independent of i and characterizes $\frac{\partial F}{\partial p_{i',j}}$ for intervals with index i' where $0 < p_{i',j} < p_{i,j}^{\max}$. Given that F is convex and increasing, and that $\frac{\partial F}{\partial p_{i,j}} \geq \frac{\partial F}{\partial p_{i',j}}$, we conclude that the power during interval M_i where by assumption job j does not charge is at least as high as during intervals where job j does charge at a (positive) power below its maximum.

Lastly, consider the case where $0 < p_{i,j} = p_{i,j}^{\max}$. Complementary slackness gives us $\gamma_{i,j} = 0$, leaving us with

$$\begin{aligned} 0 &= -\delta_j + \frac{\partial F}{\partial p_{i,j}} + \zeta_{i,j} \\ \iff \zeta_{i,j} &= \delta_j - \frac{\partial F}{\partial p_{i,j}}. \end{aligned} \quad (9)$$

Applying similar reasoning as in the previous case and considering that the signs in the right hand sides of (8) and (9) are reversed, we conclude that the power in any interval M_i where job j is executed at maximum speed, is at most as high as during intervals where j is available and is either charged at a (positive) power below its maximum, or is available and not charged at all.

From the above analysis, the following necessary and sufficient conditions for a schedule to be optimal follow:

- KKT1 The aggregated speed in all intervals where j is scheduled but does not reach its speed limit is the same.
- KKT2 The aggregated speed in intervals where j could, but does not run is at least as high as in intervals where j actually runs.
- KKT3 The aggregated speed in intervals where j runs at maximum speed is smaller or equal than in intervals where j runs below its speed limit.

The first two conditions are similar to those derived by Bansal, Kimbrel and Pruhs, whereas the last results from the addition of job-specific speed limits.

In Section III-D2 we show that the output of the FOCS algorithm introduced in Section III-C2 is a feasible schedule that satisfies said conditions. For such a schedule, we can solve the system (7), (8) and (9), proving optimality of the derived primal solution.

C. Offline algorithm using flows

In this section, we present an iterative offline algorithm to determine an optimal schedule for DSL instances, minimizing an increasing, convex and differentiable function of the aggregated speed profile. First, note that due to the convexity of the objective function and the finite number of release times and deadlines, the aggregated speed profile of any optimal solution is a step function. Moreover, the aggregated speed within any atomic interval M_i is constant for such a schedule. Similarly to YDS, the algorithm presented here uses the notion of critical intervals. These intervals are exactly those intervals that in an optimal solution require the highest aggregated power. Formally, these intervals are defined as follows.

Definition 5 (Critical intervals): An atomic interval M_i is *critical* if for any optimal schedule s its average aggregated speed $\frac{1}{|M_i|} \int_{t_i}^{t_{i+1}} \text{PF}_s(t) dt$ is larger or equal to the average aggregated speed $\frac{1}{|M_{i'}|} \int_{t_{i'}}^{t_{i'+1}} \text{PF}_s(t) dt$ for any $i' \in \mathcal{M}$.

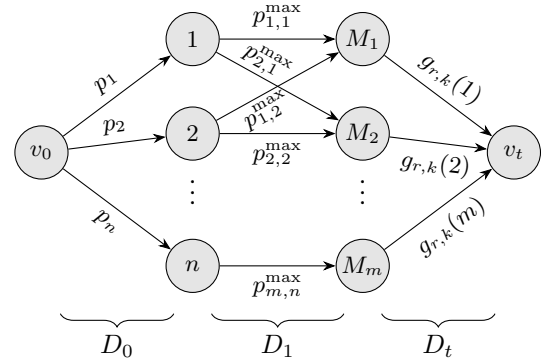


Fig. 4: Schematic of flow network structure of DSL.

Note that there may be multiple critical (atomic) intervals. Furthermore, one major difference with critical intervals as defined for YDS is that jobs do not have to be fully contained within a (set of) critical interval(s) in order to be scheduled there. This difference with YDS follows from the job-specific speed limits. The speed profile that YDS assigns to what they call a critical interval when solving DS instances is not necessarily feasible in DSL, the setting with speed limits (see e.g., Figure 2). Compared to YDS, determining critical intervals and their power level is more involved. In the algorithm presented in Section III-C2, determining critical intervals is based on the computation of multiple maximum flows. To be able to compute the flows and to keep track of the developments over the iterations of the proposed algorithm, we follow the DSL notation introduced so far, and introduce some additional notation.

1) *Flow formulation.*: For the proposed algorithm, we use a network $G = (V, D)$. The network is initialized as follows (see also Figure 4). The vertex set V consists of source and sink vertices v_0 and v_t , as well as two sets of vertices representing job vertices and atomic interval vertices respectively, i.e., $V = \{v_0, v_t\} \cup \mathcal{J} \cup \{M_i | i \in \mathcal{M}\}$. Furthermore, the edge set D consists of the union of the following three sets:

$$\begin{aligned} D_0 &= \{(v_0, j) | j \in \mathcal{J}\} \\ D_1 &= \{(j, M_i) | j \in \mathcal{J}, i \in J^{-1}(j)\} \\ D_t &= \{(M_i, v_t) | i \in \mathcal{M}\} \end{aligned}$$

with respective edge capacities

$$c_{u,v} = \begin{cases} p_v & \text{if } u = v_0, v \in \mathcal{J} \\ p_{i,u}^{max} & \text{if } u \in \mathcal{J}, v = M_i, i \in J^{-1}(u) \\ g_{r,k}(u) & \text{if } u \in \mathcal{M}, v = v_t \end{cases}$$

Note that the function $g_{r,k}$ is not defined yet. The algorithm works with rounds (indexed by r), each of which executes iterations (indexed by k). Intuitively, $g_{r,k}$ is a lower bound on the flatness of the aggregated speed profile. It varies over the execution of the algorithm, and is discussed in more detail in Section III-C2.

Given a flow f in network G , we denote the flow value as $|f|$ and call an edge (u, v) *saturated* if $f(u, v) = c_{u,v}$. Note that a flow in G corresponds to an EV schedule. Here, a job j is scheduled to process $f(j, M_i)$ units of work in interval M_i ,

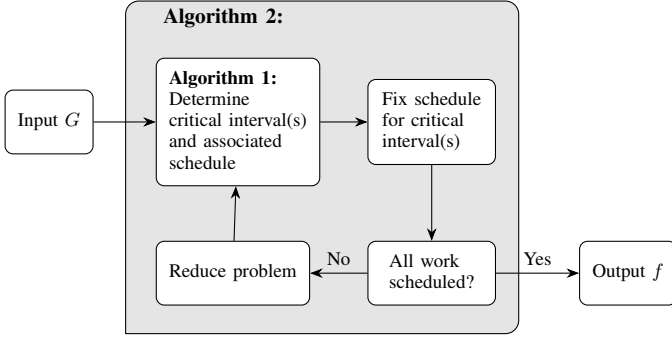


Fig. 5: Schematic overview of FOCS.

or equivalently an EV j charges $f(j, M_i)$ in interval M_i and the capacities on edges in D_1 model the job-specific speed limits. Furthermore, any flow for which the edges in D_0 are saturated corresponds to a feasible EV charging schedule and the flow through D_t models the aggregated speed in the atomic intervals of the charging schedule corresponding to f . Note that the capacities and flow through D_t are expressed in terms of the aggregated work processed. By normalizing for the length of each atomic interval, we can deduce the aggregated speed profile. Based on this correspondence, we may use the network structure to not only derive a feasible, but an optimal schedule for objective function $F(\sum_{j \in \mathcal{J}} s_j(t))$.

2) *Algorithm formulation.*: In the following, we use network G defined in Section III-C1 to derive an iterative algorithm that gives an optimal schedule and power profile for (aggregated) EV charging with an increasing, convex and differentiable objective function $F(\sum_{j \in \mathcal{J}} s_j(t))$.

Before going into detail, we provide some intuition and a rough overview of the workings of the algorithm. Intuitively, the edge set D_0 can be interpreted as the processing work of the jobs. For any feasible DSL schedule, those demands have to be met. The flow through edge set D_1 , on the other hand, is what we are trying to determine: the schedule itself. For any interval node M_i , the incoming flow corresponds to the load scheduled in that interval. In particular, $f(j, M_i)$ is the work processed for job j in interval M_i . Whereas the capacities of edges in D_0 and D_1 are determined by the instance, edge capacities of edges in D_t are not. However, the flow through D_t directly corresponds to the value of the objective function. Therefore, the algorithm presented in this section defines edge capacities for D_t such that they are a lower bound on the highest aggregated speed contributing to the objective function, i.e., a lower bound on the outgoing flow of nodes M_i where M_i is a critical interval. If given those capacities, we find a maximum flow that saturates all edges in D_0 , we have found a feasible solution with this maximum speed, and use this to determine the partial schedule for any critical interval M_i . This partial schedule corresponds to the incoming flow at each such node M_i . Else, we adapt the lower bound and repeat the process until we do find such a maximum flow and partial schedule.

In Figure 5 we provide a rough outline of an algorithm that exploits the bottleneck function of the critical intervals. In both the algorithm formulation and analysis, we distinguish

between iterations and rounds of the algorithm. In Figure 5, a new round starts every time that Algorithm 1 is called. To determine a (set of) critical interval(s) (see Definition 5), we may require multiple iterations in which we adapt the lower limit. Given the dynamic nature of this lower limit, we denote it as $g_{r,k}$ where r and k denote the current round and iteration respectively. At the end of a round, we have determined a (set of) critical interval(s). We determine the schedule for those intervals to be the incoming flow at the corresponding interval nodes. For non-critical intervals, there is no schedule yet. Their schedules will be determined in the next rounds. In that fashion, we will construct a schedule for the entire instance. To keep track of what has yet to be scheduled, we introduce the notion of *active intervals*. At the beginning of a round, interval M_i is active if it has not yet been scheduled (i.e., has not yet been critical) in previous rounds. Let \mathcal{M}_a be the set of indices of active intervals, which we initialize to be all atomic intervals, i.e., $\mathcal{M}_a = \mathcal{M}$.

The first iteration of the first round goes as follows. Given that we have to schedule a certain amount of energy and that the objective function is increasing, the most optimistic lower bound on the aggregated power is a constant profile over all intervals. Therefore, we initialize the capacities of the edges in D_t by

$$g_{1,1}(i) = \frac{\sum_{j=1}^n p_j}{L(\mathcal{M}_a)} |M_i| \quad \forall i \in \mathcal{M}_a,$$

which is the aggregated energy charged in atomic interval M_i given that in all intervals the same aggregated charging power is used, and all energy requirements are met. In that way, the edge capacities of D_t act as lower bounds to the highest aggregated power level. They are dynamic and will be increased over iterations. Given the capacities, we determine a maximum flow $f_{1,1}$ for this instance. If the flow value $|f_{1,1}|$ of $f_{1,1}$ is $\sum_{j=1}^n p_j$, we have found a feasible schedule, and all active intervals are critical. If not, then there is at least one non-saturated edge (M_i, v_t) with M_i an active interval. We call the intervals corresponding to such edges *subcritical*. Note that those intervals will not be critical in this round. We therefore temporarily remove them from the set of active intervals and add them to what we call the collection of *parked intervals* \mathcal{M}_p . At the beginning of each round, this collection is initialized to be empty. This is the end of the first iteration.

From here, we structurally increase the edge capacities of edges in D_t and again compute a maximum flow until all edges in D_0 are saturated, and we find a feasible EV schedule. To this end, first note that after the first iteration,

$$\sum_{j=1}^n c_{v_0,j} - |f_{1,1}| = \sum_{j=1}^n p_j - |f_{1,1}| > 0$$

if there were subcritical intervals. In particular, this means that there are jobs j for which additional work still needs to be scheduled. Among the interval-vertices, the only candidates for additional flow are those vertices M_i for which edge (M_i, v_t) was saturated in $f_{1,1}$, i.e., the remaining active intervals.

Keeping the objective in mind, we therefore proportionally increase the capacities at the remaining active intervals to

$$g_{1,2}(i) = g_{1,1}(i) + \frac{\sum_{j=1}^n p_j - |f_{1,1}|}{L(\mathcal{M}_a)} |M_i| \quad \forall i \in \mathcal{M}_a.$$

We repeat this process until we find a flow with flow value $\sum_{j=1}^n p_j$. Such a flow leads to a feasible EV schedule for which the maximum aggregated power is minimal. Say this happens after K_1 iterations. The remaining active intervals in that iteration make up the set of critical intervals in the corresponding round. In Figure 5, this case corresponds to the first time we leave the box of Algorithm 1 and move on to fix parts of the schedule we aim to compute.

We generalize the steps discussed thus far to an arbitrary round r and iteration k with $1 \leq k < K_r - 1$ where K_r is the number of iterations in round r . This yields:

$$g_{r,1}(i) = \frac{\sum_{j=1}^n c_{v_0,j}}{L(\mathcal{M}_a)} |M_i| \quad \forall i \in \mathcal{M}_a$$

$$g_{r,k+1}(i) = g_{r,k}(i) + \frac{\sum_{j=1}^n c_{v_0,j} - |f_{r,k}|}{L(\mathcal{M}_a)} |M_i| \quad \forall i \in \mathcal{M}_a$$

given that flow $f_{r,k}$ is the maximum flow in round r and iteration k , and that between iterations active intervals and flow networks are updated. We end the round when we find a maximum flow with flow value $\sum_{j=1}^n c_{v_0,j}$.

After each round r , we fix the part of the schedule associated with the critical interval(s) (top right box in Figure 5) to correspond to the flow incoming at the respective (critical) interval nodes, and reduce the remainder of the problem by constructing a new network G_{r+1} (bottom left box in Figure 5) as follows. First, we exploit the acyclic topology of the network to define a flow $f_r|_{M_r^*}$ of the determined maximum flow f_r , where $M_r^* = \{i \in \mathcal{M} \mid M_i \text{ is critical in round } r\}$ is the set of indices of critical intervals and

$$f_r|_{M_r^*}(M_i, v_t) = \begin{cases} f(M_i, v_t) & \text{if } i \in M_r^* \\ 0 & \text{otherwise} \end{cases}$$

$$f_r|_{M_r^*}(j, M_i) = \begin{cases} f(j, M_i) & \text{if } i \in M_r^* \\ 0 & \text{otherwise} \end{cases}$$

$$f_r|_{M_r^*}(v_0, j) = \sum_{i \in J^{-1}(j)} f_r|_{M_r^*}(j, M_i).$$

Note that this definition backpropagates flow from the sink to the source. Intuitively, $f_r|_{M_r^*}$ denotes the flow that goes through critical intervals. In the YDS-sense, $f_r|_{M_r^*}(v_0, j)$ is the critical load of job j in round r . Now, G_{r+1} is the network obtained by removing edges (M_i, v_t) with $i \in I_r^*$ from G_r , and updating edge capacities to be $c_{u,v} - f_r|_{M_r^*}(u, v)$. From here, we start the next round of the algorithm and initialize a new flow $f_{r+1,1}$. For convergence, between iterations within a round we similarly construct $G_{r,k+1}$ based on the subcritical flow $f_{r,k}|_{\mathcal{M}_p}$. Alternatively, we can require for $k \geq 1$ that we initialize flow $f_{r,k+1}$ with $f_{r,k}$ and augment it to a maximum flow using for example shortest augmenting path algorithms.

The optimal flow output by the algorithm is $f = \sum_r f_r|_{M_r^*}$. Implicitly, we use that augmenting paths in future rounds will not reshuffle the already determined subschedule induced by the

critical intervals. We will come back to that in Lemma 4. For more information about augmenting paths, and their relation to maximum flows, please refer to e.g., [16].

The algorithm to derive a feasible schedule within a round is summarized in Algorithm 1. This algorithm is then embedded in the global algorithm (Algorithm 2) described in this section, outputting a flow f corresponding to an optimal EV charging schedule. We refer to this algorithm as *Flow-based Offline Charging Scheduler* (FOCS). To illustrate, Figure 6 displays both the flow and aggregated power profile of an example instance over the rounds and iterations of the algorithm. Here, the first three flows display $f_{r,k}$, whereas the last flow is the optimal flow f . In the respective power profiles corresponding to the flow-induced schedules, shaded intervals are parked, and solid green intervals are critical. In general, maximum flows are not unique. To illustrate that, the first flow is deliberately chosen such that the flow through $(1, I_1)$ differs from that through $(1, I_3)$. Note how the optimal power profile in the bottom graph is a sum of the green components at the end of each round of the algorithm. Note that Step 10 in Algorithm 2 can be reformulated as a recursion by calling $\text{FOCS}(G_r)$.

Algorithm 1 ROUND

Input: G_r, r, \mathcal{M}_a

Output: feasible flow f_r , critical sets M_r^*

- 1: Initialize: $\mathcal{M}_p = \emptyset, k = 0, G_{r,k} = G_r$
 - 2: $c_{M_i, v_t} = g_{r,k}(i) \quad \forall i \in \mathcal{M}_a$
 - 3: Determine a maximum flow $f_{r,k}$
 - 4: $\mathcal{M}_p = \mathcal{M}_p \cup \{i \in \mathcal{M}_a \mid i \text{ subcritical in } f_{r,k}\}$
 - 5: $\mathcal{M}_a = \mathcal{M}_a \setminus \mathcal{M}_p$
 - 6: **if** $|f_{r,k}| = \sum_{j=1}^n c_{v_0,j}$ **then**
 - 7: **return** $f_r = f_{r,k}, M_r^* = \mathcal{M}_a$
 - 8: **else**
 - 9: $G_{r,k+1} = G_{r,k}$ with capacities reduced by $f_{r,k}|_{\mathcal{M}_p}$ and vertices M_i removed for subcritical M_i
 - 10: $k = k + 1$ and repeat from Step 2
 - 11: **end if**
-

Algorithm 2 FOCS

Input: G

Output: optimal flow f

- 1: Initialize: $\mathcal{M}_a = \mathcal{I}, \mathcal{M}_p = \emptyset, r = 0, G_r = G, f$
 - 2: $f_r, M_r^* = \text{ROUND}(G_r, r, \mathcal{M}_a)$
 - 3: $\mathcal{M}_a = \mathcal{M}_a \setminus M_r^*$
 - 4: $f = f + f_r|_{M_r^*}$
 - 5: $G_{r+1} = G_r$ with capacities reduced by $f_r|_{M_r^*}$ and vertices M_i removed for $i \in M_r^*$
 - 6: $r = r + 1$
 - 7: **if** $\mathcal{M}_a = \emptyset$ **then**
 - 8: **return** f
 - 9: **else**
 - 10: Repeat from Step 2
 - 11: **end if**
-

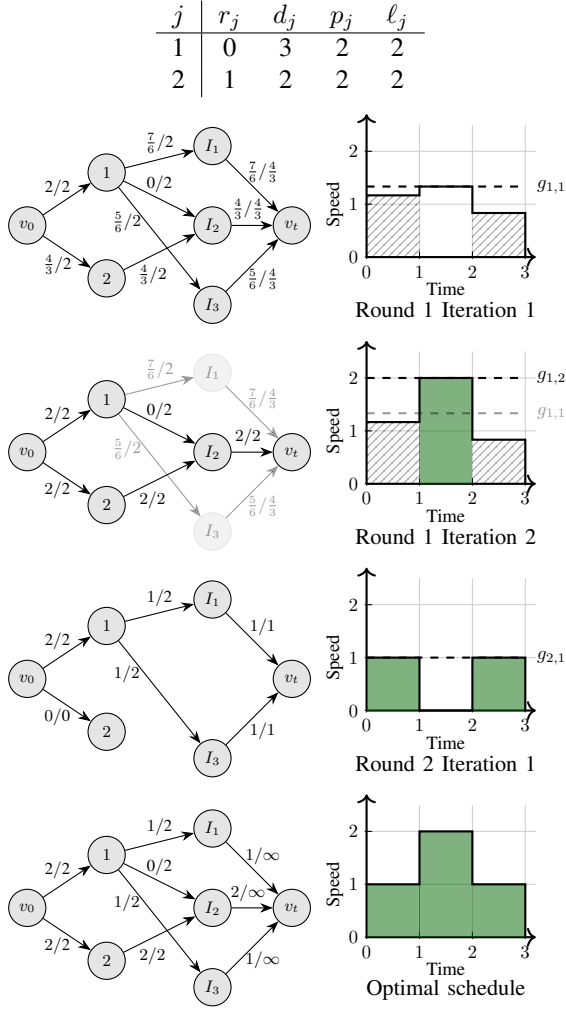


Fig. 6: Intermediate states of FOCS for an example instance, tracked over rounds and iterations.

D. Algorithm analysis

In this section, we analyze FOCS, the algorithm presented above. In particular, Section III-D1 shortly discusses its time complexity and properties, after which its optimality is proved in Section III-D2.

1) *Properties and time complexity.*: In this section, we discuss some properties and lemmas that apply to the flow model and algorithm. In particular, we establish some building blocks that enable us to prove optimality of the algorithm in Section III-D2.

Lemma 2: If an instance has a feasible schedule, FOCS terminates and outputs a feasible schedule. Its time complexity is bound by $\mathcal{O}(n^2\mu)$ where $\mathcal{O}(\mu)$ is the time complexity of the used maximum flow algorithm.

Proof of Lemma 2: First, we argue that FOCS terminates and analyze its time complexity. We do this by arguing that the number of iterations in Algorithm 1, and the number of rounds in Algorithm 2 calling Algorithm 1 are finite.

Any feasible schedule s can be directly translated to a feasible flow for G_r by sending $\int_{t_i}^{t_{i+1}} s_j(t) dt$ units of flow through edge (j, M_i) for each job j and $i \in J^{-1}(j)$. The flows through edges in D_0 and D_t follow directly by flow

conservation. Therefore, there exists a maximum flow for the input to Algorithm 1 which saturates all edges in D_0 . The algorithm (and therefore the current round) finishes once the if condition in Step 6 is satisfied, i.e., if we find a maximum flow that saturates all edges outgoing of sink node v_0 when using edge capacities $g_{r,k}$ for the network. If Step 6 is false, there exists at least one subcritical interval M_i for which the flow through (M_i, t) is strictly below capacity $g_{r,k}(i)$. In each iteration, at least one such interval is removed from the network, until $g_{r,k}$ is increased sufficiently to find a maximum flow satisfying the if condition. The number of intervals is finite, and therefore the number of iterations in Algorithm 1 is finite. In particular, we can bound this number to at most $2n - 1$ iterations per round, based on the fact that the number m of atomic intervals is bound by the number of jobs j , implying that $m \leq 2n$. Note that there are efficient algorithms available to solve maximum flow problems, e.g., [16]–[19]. Furthermore, a comprehensive overview of traditional polynomial time maximum flow algorithms is given by [20]. Denoting their time complexity by μ , we find that Algorithm 1 has a time complexity of $\mathcal{O}(n\mu)$.

As at the end of each round at least one interval is critical and therefore removed from \mathcal{M}_a , the finite number of intervals implies that the if condition in Step 7 of Algorithm 2 is satisfied after at most $2n - 1$ rounds, and hence FOCS terminates. This implies that the time complexity of FOCS is bound by $\mathcal{O}(n^2\mu)$.

Note that the time complexity for the EV charging setting may be reduced further by exploiting the underlying structure of EV charging schedules, and by considering the decrease in network size over the rounds of the algorithm. In particular, we may initialize the flow of any iteration with the flow found in the previous iteration of the same round. Furthermore, there are maximum flow algorithms that are cubic in the number of nodes [20]. As the largest flow network that is considered in FOCS (the network in the initial round) has $n + m + 2 \leq 3n + 2$ nodes, a rough upper bound of the time complexity of maximum flows in FOCS is given by $\mu \leq n^3$.

Finally, feasibility of the output follows from the defined edge capacities of the considered network. Following the order of DSL feasibility conditions listed in Definition 1, we conclude that:

- (i) Every job j is fully processed within its availability since by flow conservation the exact amount of work done per job within its availability is the flow through edge (v_0, j) . The algorithm only terminates once that edge is saturated, i.e., if $f(v_0, j) = p_j$.
- (ii) An edge (j, M_i) is in D_1 if and only if $j \in J(i)$. Therefore, assuming the default value is zero, all decision variables $e_{i,j}$ for which $i \in \mathcal{M} \setminus J^{-1}(j)$ are zero, implying that the speed of j outside its availability is zero.
- (iii) Each job respects its speed limit by the capacities defined for edges in D_1 .

Therefore, the output of FOCS is feasible. \blacksquare

Next, we extend on the concept of work-transferability as described by [10] to integrate job-specific speed limits.

Definition 6 (Work-transferability): If for a given schedule and atomic intervals M_i and $M_{i'}$ there exists a job $j \in J(i) \cap J(i')$ such that $p_{i,j} > 0$ and $p_{i',j} < p_{i',j}^{\max}$, we state that the

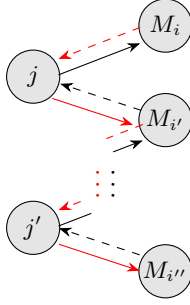


Fig. 7: Work-transferability represented in flows.

work-transferable relation $i \rightarrow i'$ holds. Furthermore, let \rightarrow be the transitive closure of \rightarrow .

Intuitively, if we have work-transferability from one atomic interval i to another atomic interval i' , then we can transfer some work that was scheduled during i to i' . In EV charging terms this implies that we can advance or delay some charging from one period in time to another. Applying the concept to flows, we can make the following statement.

Lemma 3 (Work-transferability in flows): For a given schedule and atomic intervals M_i and $M_{i'}$, we have $i \rightarrow i'$ if and only if there exists a path $(M_i, j, M_{i'})$ in the residual graph corresponding to the schedule, where $j \in \mathcal{J}$. Similarly, we have $i \rightarrow i''$ if and only if in the residual network corresponding to the schedule there exists an $(M_i - M_{i''})$ -path through interval and job vertices only.

Proof of Lemma 3: We show only the first statement as the extension follows naturally using concatenations of paths. Assume that $i \rightarrow i'$. Then there exists a job j such that $j \in J(i) \cap J(i')$ with $p_{i,j} > 0$ and $p_{i',j} < p_{i',j}^{\max}$. The former implies that edge (M_i, j) exists in the residual graph. As $c_{j,M_{i'}} = p_{i',j} < p_{i',j}^{\max}$, edge $(j, M_{i'})$ is in the residual graph. This proves existence of path $(M_i, j, M_{i'})$ in the residual graph.

For the opposite direction, assume the existence of a path $(M_i, j, M_{i'})$. Since $j \in \mathcal{J}$, we know the edge capacity $c_{j,M_{i'}}$ in the original network to be $p_{i',j}^{\max}$. The existence of the edge in the residual graph implies that for the flow going through this edge which is defined by the schedule to be $p_{i',j}$, we have $p_{i',j} < p_{i',j}^{\max}$. Furthermore, existence of edge (M_i, j) in the residual graph indicates positive flow through (j, M_i) in the original network, implying $p_{i,j} > 0$. From the presence of both edges, it follows that $j \in J(i) \cap J(i')$, proving that $i \rightarrow i'$. ■

Figure 7 illustrates the concept of work-transferability. Here, dashed edges are those that are not in the original network, but might be present in the residual network. Lemma 3 translates work-transferability to the existence of (in the figure) red paths in the residual network.

Next, we consider two lemmas that have a more direct relation to the algorithm.

Lemma 4 (Isolation of critical intervals): If M_i is a critical interval in round r and if the round consists of multiple iterations whereby $M_{i'}$ was subcritical in one of those iterations, then there is no work-transferable relation between i and i' in the schedule corresponding to the flow at the end of round r , i.e., $i \not\rightarrow i'$ with respect to flow f_r .

Proof of Lemma 4: We prove the lemma by constructing an

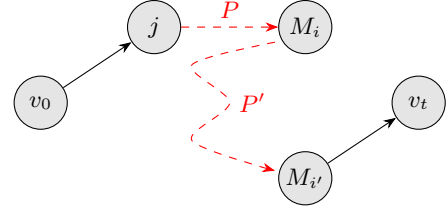


Fig. 8: Illustration of augmenting path in proof of Lemma 4.

augmenting path (see Figure 8). Assume in round r interval $M_{i'}$ was parked in iteration k and let $f_{r,k}$ be the flow at the end of iteration k . Since $M_{i'}$ is subcritical, we have $|f_{r,k}| < \sum_{j=1}^n p_j$, implying that for the next iteration the lower bound $g_{r,k}$ will be increased to

$$g_{r,k+1}(i'') = g_{r,k}(i'') + \frac{\sum_{j=1}^n c_{v_0,j} - |f_{r,k}|}{L(\mathcal{M}_a)} |M_{i''}| \quad \forall i'' \in \mathcal{M}_a.$$

By criticality of M_i , the interval is active at the end of the iteration, implying $g_{r,k+1}(i) > g_{r,k}(i)$. Furthermore, criticality implies that there is no iteration in this round where M_i is subcritical. Combing those facts, the flow through (M_i, t) increases in iteration $k+1$ compared to iteration k . This is only possible if there is a job j such that (v_0, j) is not saturated and there exists a $(j - M_i)$ -path P in the residual graph. Furthermore, note that since $M_{i'}$ is being parked in iteration k , edge $(M_{i'}, t)$ is not saturated and therefore exists in the residual graph. Now, assume $i \rightarrow i'$. By Lemma 3, there exists an $(M_i - M_{i'})$ -path P' that passes only through job and interval vertices. This implies that $P'' = (v_0, P, P', v_t)$ exists in the residual graph and contains an $(v_0 - v_t)$ -path, proving existence of an augmenting path in $f_{r,k}$. This contradicts maximality of the flow, implying $i \not\rightarrow i'$. ■

Intuitively, this lemma says that we cannot push any charging from (high power) critical intervals to (low power) subcritical intervals. This is in line with the notion of critical intervals as introduced for the YDS algorithm, and will be a key element in the optimality proof in Section III-D2. Furthermore, this particular lemma justifies that we fix the schedule of critical intervals at the end of each round.

For the next lemma, we first introduce the notion of ranks.

Definition 7 (Rank): The rank $r(i)$ of an atomic interval M_i is defined as the round $r(i)$ in which M_i was critical, i.e., $i \in M_{r(i)}^*$.

Lemma 5 (Monotonicity): For the schedule corresponding to output flow f of algorithm FOCUS and atomic intervals M_i and $M_{i'}$ where $r(i) < r(i')$, the aggregated power in M_i is strictly larger than in $M_{i'}$, i.e.,

$$\frac{f(M_i, t)}{|M_i|} > \frac{f(M_{i'}, t)}{|M_{i'}|}$$

Proof of Lemma 5: We prove the lemma by contradiction, whereby we consider flows at the end of rounds. Let interval M_i be the lowest ranked interval such that its aggregated power level in the flow outputted by the algorithm is larger than that in intervals with rank $r(i) - 1$. As the algorithm does not change schedules at critical intervals, this already occurs at

round $r(i)$ itself. Given that M_i was subcritical in the previous round, the speed level for M_i increased. In particular, there is a job j for which the speed during interval M_i increased compared to the previous round. Furthermore, we know that the flow through (j, M_i) is positive in round $r(i)$, implying that edge (M_i, j) is in the residual graph. However, applying Lemma 4 to the previous round, the amount of work scheduled for job j remains the same. Therefore, there is an interval $M_{i'}$ for which the flow through $(j, M_{i'})$ decreased compared to the previous round. As a consequence, the flow in round $r(i)$ does not saturate the edge, implying that edge $(j, M_{i'})$ is in the residual graph. Combining these findings, the path $(M_i, j, M_{i'})$ is in the residual graph, implying $i \rightarrow i'$, and thus contradicting Lemma 4. ■

The lemma shows that the average aggregated speed of atomic intervals is decreasing in their rank. Therefore, critical intervals as determined using the method presented in this paper share the monotonicity property known for YDS for corresponding DS instances. We first find those intervals with the highest intensity, and then iteratively determine the next highest speeds.

We also note that, similarly to YDS, the power profile outputted by FOCS is unique if the objective function is strictly convex. However, this does not necessarily apply to the schedule.

2) *Optimality proof.*: In this section, we prove that Algorithm 2 as described in Section III-C2 is optimal for any increasing, convex and differentiable objective function $F(\sum_{j \in \mathcal{J}} s_j(t))$. To this end, we first prove some auxiliary lemmas that show compliance with the sufficient conditions derived in Section III-B.

Lemma 6: The output of Algorithm 2 complies with KKT1.

Proof of Lemma 6: If in the final output of the algorithm there are two distinct atomic intervals M_i and $M_{i'}$ such that for job j we have $0 < \frac{p_{i,j}}{|M_i|} = \frac{p_{i',j}}{|M_{i'}|} < \ell_j$, then by definition of worktransferability we have $i \rightarrow i'$ and $i' \rightarrow i$. By Lemma 4 and the strict monotonicity in Lemma 5, this implies that the aggregated speed in both intervals is the same. ■

Lemma 7: The output of Algorithm 2 complies with KKT2.

Proof of Lemma 7: Let $i \in J^{-1}(j)$ be such that $p_{i,j} = 0$ in the output of the algorithm. Assume that there is an interval $M_{i'}$ with $i \neq i'$ and $i' \in J^{-1}(j)$ for which the aggregated power in $M_{i'}$ is strictly greater than in M_i , i.e., $\frac{\sum_{j=1}^n p_{i,j}}{|M_i|} < \frac{\sum_{j=1}^n p_{i',j}}{|M_{i'}|}$. By Lemma 5 we have $r(i') < r(i)$, implying by Lemma 4 that $i' \not\rightarrow i$. Applying the definition of work-transferability, it follows that $p_{i',j} = 0$, proving compliance with KKT2. ■

Lemma 8: The output of Algorithm 2 complies with KKT3.

Proof of Lemma 8: Let job j run at maximum speed in M_i in the schedule found by FOCS. Assume that there is an interval $M_{i'}$ with $i \neq i'$ and $i' \in J^{-1}(j)$, such that the aggregated speed in M_i is strictly greater than in $M_{i'}$. By Lemma 5, we know that $r(i) < r(i')$. Therefore, by Lemma 4, there is no work-transferable relation between i and i' ($i \not\rightarrow i'$). From the definition of work-transferability it now follows directly that $p_{i',j} \geq p_{i',j}^{\max}$, proving compliance with KKT3. ■

Combining all discussed above, we conclude optimality of the algorithm output.

Theorem 9 (Optimality): For any feasible input instance, the schedule produced by Algorithm 2 is an optimal solution minimizing any convex, increasing and differentiable objective function of the aggregated output powers.

Proof of Theorem 9: The proof follows directly from the KKT conditions derived in Section III-B, the inherent feasibility of the output and Lemmas 6–8. ■

To summarize, this section considered the offline DSL problem, applicable to EV scheduling in MPC settings. In particular, we analyzed the relation between solutions of DSL instances and their corresponding DS instances. Furthermore, we derived necessary and sufficient optimality conditions for DSL schedules and presented an offline algorithm that determines an optimal schedule in $\mathcal{O}(n^2\mu)$ time where μ is the complexity of an efficient maximum flow algorithm. Lastly, we provided proof of the optimality of the output of the algorithm.

IV. ONLINE SCHEDULING

As discussed in the introduction, MPC is a much-deployed framework for coordinated EV charging, especially due to its usability to bridge data gaps. However, it is an interesting and important question to ask how close to an optimal solution such frameworks can get, and in particular, how close to optimal an MPC, or intraday controller, can get, assuming perfect knowledge on an EV's characteristics upon arrival. Note that in that case, the model-component of the MPC was clairvoyant.

Also from a theoretical point of view, considering DSL in an online setting is a natural next step. Therefore, in this section, we are interested in schedules constructed *online*, i.e., schedules where jobs are released one by one, and the algorithm only gets to know their characteristics at their respective release times.

A. Preliminaries online algorithms

We define the online variant of a job scheduling problem to be such that the existence and characteristics of jobs become known at their respective release times. In this section, we analyze online algorithms for DSL in terms of their respective *competitive ratio*.

Definition 8: Given a deterministic algorithm ALG that for any DSL instance $I \in \mathcal{I}_{DSL}$ determines a feasible schedule $s^{\text{ALG}}(I)$, and given an optimal solution $s^*(I)$, the *competitive ratio* of the algorithm is defined as

$$\sup_{I \in \mathcal{I}_{DSL}} \frac{E(s^{\text{ALG}}(I))}{E(s^*(I))}. \quad (10)$$

The definition carries over to DS instances.

Two classical online approaches for DS are Average Rate (AVR) and Optimal Available (OA) [8]. Given the connection between DSL and DS, we first provide a short description of those two algorithms, before relating them to DSL.

1) AVR.: AVR for DS works in two steps. First, upon release, job j is scheduled at speed $\frac{p_j}{d_j - r_j}$ throughout its availability, i.e., each job is scheduled at the constant speed corresponding to the average speed it needs to complete its work between release time and deadline. The resulting schedule may not be feasible for DS, since jobs may run simultaneously, but it gives

a useful initial speed profile. Therefore, in a second step, EDF is applied using the speed profile resulting from the initial schedule.

2) OA.: OA reoptimizes the remaining problem instance each time a new job is released. In particular, let s be an optimal schedule for jobs $\mathcal{J} = \{1, \dots, n\}$ and instance $I = \langle \vec{r}, \vec{d}, \vec{p} \rangle$. Let t' be the first point in time where a new job $n+1$ is released. We then define the remaining instance at point t' according to schedule s as $I' = \langle \vec{r}', \vec{d}', \vec{p}' \rangle$ where:

$$\begin{aligned} \vec{r}'_j &= t' & \forall j \in \mathcal{J} \cup \{n+1\} \\ \vec{d}'_j &= d_j & \forall j \in \mathcal{J} \cup \{n+1\} \\ \vec{p}'_j &= \begin{cases} p_j - \int_{r_j}^{t'} s_j(t) dt & \text{if } j \in \mathcal{J} \\ p_{n+1} & \text{if } j = n+1. \end{cases} \end{aligned}$$

For convenience, if a job has remaining workload 0 or if its deadline is at most t' , we remove it from the remaining problem instance. We now determine an optimal schedule s' for I' . The updated schedule \bar{s} for OA at time t' is such that

$$\bar{s}_j(t) = \begin{cases} s_j(t) & \text{if } j \in \mathcal{J} \wedge t < t' \\ s'_j(t) & \text{if } j \in \mathcal{J} \wedge t \geq t' \\ s'_{n+1}(t) & \text{if } j = n+1. \end{cases}$$

Iteratively repeated over the time horizon every time a new job is released, this results in a schedule s_{OA} for OA.

Note that OA may be applied to either DS or DSL, with the difference being the algorithm applied in the optimization subroutine. Optimization for DS may be done by applying YDS, whereas for DSL FOCS is a suitable optimization algorithm.

B. Average Rate for DSL

In the following, we discuss the application of AVR to DSL instances. As remarked earlier, EDF does not necessarily result in a feasible schedule for DSL instances, even if it follows a profile for which there exists a feasible schedule (see Figure 3). However, since feasible schedules for DSL allow more than one job to be processed at any time and since by assumption (3) holds, we can adapt AVR to DSL instances by skipping the last step (therefore not applying EDF) to find a feasible schedule. In other words, upon release, we schedule any job j at speed $\frac{p_j}{d_j - r_j}$ for the next $d_j - r_j$ units of time.

We analyze the performance guarantee of applying AVR to DSL instances by relating the resulting schedules to those resulting from applying AVR to DS instances as follows. Assume we are given an instance $I = \langle \vec{r}, \vec{d}, \vec{p}, \vec{\ell} \rangle$. Let $s^{\text{DSL,AVR}}$ be the schedule for I found by AVR without EDF and let $s^{\text{DSL,*}}$ be an optimal schedule. Furthermore, let $s^{\text{DS,AVR}}$ be the schedule for the corresponding augmented DS instance $a(I)$ found by AVR with EDF, and let $s^{\text{DS,*}}$ be an optimal schedule for $a(I)$. Note that $\text{PF}_{s^{\text{DS,AVR}}} = \text{PF}_{s^{\text{DSL,AVR}}}$ and therefore their objective values are the same. Thus,

$$E(s^{\text{DSL,AVR}}) = E(s^{\text{DS,AVR}}) \quad (11a)$$

$$\leq 2^{\alpha-1} \alpha^\alpha E(s^{\text{DS,*}}) \quad (11b)$$

$$\leq 2^{\alpha-1} \alpha^\alpha E(s^{\text{DSL,*}}). \quad (11c)$$

Here, (11a) follows from the fact that the AVR (respectively with and without EDF) schedules $s^{\text{DS,AVR}}$ and $s^{\text{DSL,AVR}}$ have the same speed profile, (11b) follows from the known tight competitive ratio for AVR with EDF for DS instances [13] and Lemma 1, and (11c) follows from Corollary 1.

Furthermore, we can conclude that the upper bound on the competitive ratio for AVR without EDF for DSL instances is the same as the upper bound for the competitive ratio for AVR with EDF for DS instances. In particular, assume that $I' = \langle \vec{r}, \vec{d}, \vec{p} \rangle$ was an instance for which the inequality in (11b) is an equality. Based on this, we can construct an instance I for DSL such that $a(I) = I'$ by taking $\ell_j = \max_t \text{PF}_{s^{\text{DS,*}}}(t)$. Then, the energy of the respective optimal schedules of I and I' are the same.

C. Optimal Available for DSL

In this section, we adapt the potential function approach that Bansal, Kumar and Pruhs used to analyze the competitive ratio of OA for DS instances [13] to analyze OA for DSL instances. In particular, we show the competitive ratio of α^α to be tight, where α is the same as in the energy function defined in (2). Notably, the competitive ratio for DS and DSL instances is the same.

First, we remark that while in each re-optimization step of OA there is a unique aggregated speed profile, the schedule is not necessarily unique. Therefore, we explicitly note that throughout the upcoming analysis, we consider a fixed (arbitrary) realization of OA.

Next, we introduce some notation, before giving the potential function, and deriving the competitive ratio. Let $\text{PF}_{\text{OA}}(t)$ be the aggregated speed at which OA runs at time t , and similarly let $\text{PF}_{\text{OPT}}(t)$ be the aggregated speed at which OPT runs at time t , where OPT is an optimal algorithm leading to an optimal (offline) schedule s_{OPT} . Note that these are the speed profiles as realized at the end of the time horizon and that OA recomputes a schedule every time a new task is released. Therefore, for current time t_0 , we introduce schedule s and corresponding speed $\text{PF}_s(t)$, at which OA runs at time $t \geq t_0$ if no new jobs are released after t_0 . While it holds that $\text{PF}_s(t_0) = \text{PF}_{\text{OA}}(t_0)$, this is generally not the case for $t > t_0$, since a job may be released in interval (t_0, t) .

At this point t_0 , OA may be interpreted to solve a DSL instance where all tasks have the same release time t_0 . Therefore, the resulting speed profile $\text{PF}_s(t)$ for $t > t_0$ is a non-increasing step function. Let t_1 be the first point in time after t_0 where a step occurs and the speed profile changes, i.e.,

$$t_1 = \sup\{t \geq t_0 \mid \text{PF}_s(t) = \text{PF}_s(t_0)\}.$$

Applying this inductively, we find breakpoints t_i for $i \geq 0$, such that $[t_i, t_{i+1})$ are the inclusion maximal intervals with constant speed profiles. As [13], we call such intervals *critical*, and define $M_i := [t_i, t_{i+1})$. Note that both criticality and the intervals M_i are being redefined here, as compared to their use in the offline Section III.

We define $w_{\text{OA}}(t, t')$ as the work done by OA in interval $(t, t']$ that is already available (and unfinished) at current time t_0 . Moreover, let $\frac{w_{\text{OA}}(t, t')}{t' - t}$ be the density of interval $(t, t']$. We

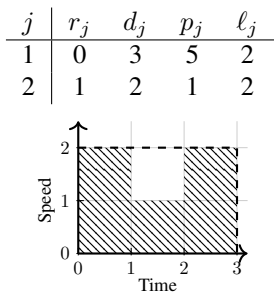


Fig. 9: Example of an instance where the speed profile corresponding to available work w_{OPT} at time $t_0 = 0$ (profile of shaded area) is not a non-increasing step function. The dashed line corresponds to the optimal speed profile at the end of the time horizon.

note that this definition of w is different from the one given by [13], to account for the methods needed to solve DSL. For critical intervals M_i , we can relate this work load to the speed profile by

$$\text{PF}_s(t) = \frac{w_{\text{OA}}(t_i, t_{i+1})}{t_{i+1} - t_i}$$

for $t \in M_i$. For notational purposes, we shorten $w_{\text{OA}}(t_i, t_{i+1})$ to $w_{\text{OA}}(i)$ in places where t_i and t_{i+1} are clear from the context.

Similarly to w_{OA} , we define $w_{\text{OPT}}(t, t')$ to be the work done by optimal schedule OPT in interval (t, t') that is already available at current time t_0 . Note that as opposed to OA, OPT is aware of tasks that will be released in the future. Therefore, the speed profile induced by w_{OPT} is not necessarily non-increasing, as shown in Figure 9. The figure shows the part of the optimal speed profile corresponding to jobs that are already available. In the middle, there is a valley in the profile, where the second (not yet available) job will be scheduled. Moreover, note that the breakpoints determined based on $\text{PF}_s(t)$ above do not necessarily align with changes in speed in the (partial) speed profile of OPT.

Finally, we define the potential function at current time $t = t_0$ to be

$$\Phi(t) = \alpha \sum_{i \geq 0} \text{PF}_s(t_i)^{\alpha-1} (w_{\text{OA}}(i) - \alpha w_{\text{OPT}}(i)).$$

Note that breakpoints t_i on the right hand side of the formula depend on function input t . Furthermore, note that the form of the introduced potential function is similar to the potential function used by [13] to derive the competitive ratio for OA under DS. The main differences lie in the problem definition, and in the definition of w_{OA} and w_{OPT} . The proof for DSL follows the same structure as that for DS presented by [13]. However, it is not evident that the same form of potential function applies to DSL. Therefore, we work out the details in places where speed limits play a role and include the proof for DSL despite the similarities.

In the following we show that:

Lemma 10: The potential function $\Phi(t)$ satisfies the following conditions:

- 1) *Boundary property:* $\Phi(t) = 0$ for any t before the first release time and for any t after the last deadline.

- 2) *Job release and completion property:* At any time t where a new task is released, or a task is completed by s_{OPT} or s_{OA} , the potential function is non-increasing, i.e.,

$$\lim_{t' \uparrow t} \Phi(t') \geq \lim_{t' \downarrow t} \Phi(t'). \quad (12)$$

- 3) *General property:* For a time t at which no job is released, we have

$$\text{PF}_{\text{OA}}(t)^\alpha + \frac{d\Phi(t)}{dt} \leq \alpha^\alpha \text{PF}_{\text{OPT}}(t)^\alpha. \quad (13)$$

[21] have previously proven similar properties for the potential function of another speed scaling model to derive the corresponding competitive ratio. The proof of Lemma 10 uses the following lemma taken from [13]. We refer to the original paper for its proof.

Lemma 11: (Lemma 3.3 in [13]): Let $q, r, \delta \geq 0$ and $\alpha \geq 1$. Then $(q + \delta)^{\alpha-1}(q - \alpha r - (\alpha - 1)\delta) - q^{\alpha-1}(q - \alpha r) \leq 0$.

Proof of Lemma 10: We consider each property separately.

For Property 1, note that for any t before the first release, or after the last deadline, there will be no tasks to schedule for OA, resulting in speed $\text{PF}_s(t_i) = 0$ for all $i \geq 0$. Hereby, $\Phi(t) = 0$ for such t .

For Property 2, we first consider the case where a new job is released. Assume task j is released at time t_0 with deadline $d_j \in M_i$, requiring an amount x of work. This release may affect the breakpoints of the critical intervals. Note that the speed profile $\text{PF}_s(t)$ before the release was a non-increasing step function. To add a job, we add its associated work to the latest intervals for which the job is available. We consider the addition of work in increments, i.e., we add some $x' \leq x$ of work until one of the following cases occurs:

- The speed in M_i increases to the speed in M_{i-1} . In particular $\text{PF}_s(t_i) = \frac{w(t_i, t_{i+1}) + x'}{t_{i+1} - t_i} = \text{PF}_s(t_{i-1})$.
- Two critical intervals M_i and M_{i+1} merge into one new critical interval.
- The speed at which job j runs in interval M_i reaches the job-specific speed limit ℓ_j .
- The interval M_i splits in two critical intervals $M_{i'}$ and $M_{i''}$. This may occur due to deadlines that do not match the already existing breakpoints, or due to speed limits being reached in parts of recently merged critical intervals.
- The job is completely scheduled (i.e., $x' = x$).

Due to the speed limits, we have to carefully keep track of the added work x' so far, before adding the next part of the work, until the whole amount of work x is scheduled.

We start with cases that do not change the structure of critical intervals. Those are the cases where M_i increases to the speed in M_{i-1} , where in M_i job j reaches its job-specific speed limit ℓ_j , and where the remaining work can be scheduled within M_i without triggering any of the other events.

By definition, OA schedules all additional work x' during M_i . Therefore, the only values associated with OA that change are $\text{PF}_s(t)$ for $t \in M_i$ and $w_{\text{OA}}(i)$. For the optimal schedule OPT, no such claim can be made. Therefore, we denote $x'_{i'} \geq 0$ to be the work scheduled for interval $M_{i'}$ for $0 \leq i' \leq i$ where $\sum_{i'=0}^i x'_{i'} = x'$.

We initially consider the i^{th} term of the potential function separately. Speed function $\text{PF}_s(t)$ changes by $\frac{x'}{t_{i+1} - t_i}$ for

$t \in M_i$. To compare the change in potential function, we denote the new speed as

$$\text{PF}_{s'}(t) = \begin{cases} \frac{w_{\text{OA}}(i)+x'}{t_{i+1}-t_i} & \text{if } t \in M_i \\ \text{PF}_s(t) & \text{otherwise.} \end{cases} \quad (14)$$

We further note that $w_{\text{OA}}(i)$ increases by x' , and $w_{\text{OPT}}(i)$ increases by x'_i . That gives a total change of

$$\begin{aligned} & \text{PF}_{s'}(t_i)^{\alpha-1} (w_{\text{OA}}(i) + x' - \alpha (w_{\text{OPT}}(i) + x'_i)) \\ & - \text{PF}_s(t_i)^{\alpha-1} (w_{\text{OA}}(i) - \alpha w_{\text{OPT}}(i)) \end{aligned} \quad (15)$$

for the i^{th} term. In the term for $i' \in \{0, \dots, i-1\}$, the values $w_{\text{OA}}(i')$ do not change after adding work x' since the work is added to a different interval, namely M_i . However, $w_{\text{OPT}}(i')$ increases by x'_i . If we sum the change for all such i' , we find the following expression:

$$\begin{aligned} & \sum_{i'=0}^{i-1} (\text{PF}_s(t_{i'})^{\alpha-1} (w_{\text{OA}}(i') - \alpha (w_{\text{OPT}}(i') + x'_{i'}))) \\ & - \text{PF}_s(t_{i'})^{\alpha-1} (w_{\text{OA}}(i') - \alpha w_{\text{OPT}}(i')) \\ & = \sum_{i'=0}^{i-1} \text{PF}_s(t_{i'})^{\alpha-1} (-\alpha x'_{i'}). \end{aligned} \quad (16)$$

To show that (12) holds in the release case, we denote $\Delta\Phi(t) = \lim_{t' \uparrow t} \Phi(t') - \lim_{t' \downarrow t} \Phi(t')$. We bring all terms together and conclude:

$$\Delta\Phi(t_0) \quad (17)$$

$$= \sum_{i'=0}^{i-1} \text{PF}_s(t_{i'})^{\alpha-1} (-\alpha x'_{i'}) \quad (18)$$

$$\begin{aligned} & + \text{PF}_{s'}(t_i)^{\alpha-1} (w_{\text{OA}}(i) + x - \alpha (w_{\text{OPT}}(i) + x'_i)) \\ & - \text{PF}_s(t_i)^{\alpha-1} (w_{\text{OA}}(i) - \alpha w_{\text{OPT}}(i)) \\ & \leq \text{PF}_{s'}(t_i)^{\alpha-1} (w_{\text{OA}}(i) + x - \alpha (w_{\text{OPT}}(i) + \sum_{i'=0}^i x'_{i'})) \end{aligned} \quad (19)$$

$$\begin{aligned} & - \text{PF}_s(t_i)^{\alpha-1} (w_{\text{OA}}(i) - \alpha w_{\text{OPT}}(i)) \\ & = \text{PF}_{s'}(t_i)^{\alpha-1} (w_{\text{OA}}(i) + x - \alpha (w_{\text{OPT}}(t_i, t_{i+1}) + x')) \\ & - \text{PF}_s(t_i)^{\alpha-1} (w_{\text{OA}}(i) - \alpha w_{\text{OPT}}(i)) \end{aligned} \quad (20)$$

$$\leq 0.$$

Here, (18) follows from the derivations in (15) and (16). In (19), we made use of the fact that for all $0 \leq i' < i$, we can lower bound the speed $\text{PF}_s(t_{i'})$ by the new speed $\text{PF}_{s'}(t_i)$. By doing so, we can exploit that $\sum_{i'=0}^i x'_{i'} = x'$ in the next step. Moreover, (20) is exactly the case discussed in the proof of Theorem 3.4 by [13] where they do inequality manipulations, apply Lemma 11 (Lemma 3.3 in [13]) and conclude non-positivity. For the details, we refer the reader to that work.

Both for the cases where interval M_i either splits in two, or merges with another, at that point the densities between old and new intervals are constant, leaving the potential function unchanged.

We conclude, that the potential function does not increase if a new task is released.

Next, consider the case where OA finishes a (at least one) task at time t . Either

$$\lim_{t' \uparrow t} \text{PF}_s(t') = \lim_{t' \downarrow t} \text{PF}_s(t'), \quad (21)$$

in which case the task finished strictly within the critical interval, leaving $\text{PF}_s(t)$ unaffected and continuously reducing $w_{\text{OA}}(t_0, t_1)$ by which (12) holds by continuity in t , or the equality in (21) does not hold, in which case we transition from one critical interval to the next. Then, indices shift by one, $\text{PF}_s(t_1)$ becomes $\text{PF}_s(t_0)$ etc. For the potential function, the only change is the formerly first term $\alpha \text{PF}_s(t_0)^{\alpha-1} (w_{\text{OA}}(t_0, t_1) - \alpha w_{\text{OPT}}(t_0, t_1))$ disappearing. However, while $\text{PF}_s(t_0)$ remained constant, both $w_{\text{OA}}(t_0, t_1)$ and $w_{\text{OPT}}(t_0, t_1)$ approached zero. The first term's contribution therefore approaches zero from above as the critical interval draws to an end. The change in potential function in such a point is therefore continuous and (12) holds.

For the case where at time t , OPT finishes a task, we note that the potential function is independent of $\text{PF}_{\text{OPT}}(t)$, and the change in $w_{\text{OPT}}(t_0, t_1)$ is continuous.

Combining the observations above, we have shown that $\Phi(t)$ satisfies Property 2.

Lastly, we show that $\Phi(t)$ has Property 3 by showing that

$$\text{PF}_{\text{OA}}(t)^\alpha - \alpha^\alpha \text{PF}_{\text{OPT}}(t)^\alpha + \frac{d\Phi(t)}{dt} \leq 0. \quad (22)$$

We consider the working case where in the next infinitesimally small dt time units no new task is released or completed by either OA or OPT. Furthermore, we do assume that there are tasks available, and that therefore $\text{PF}_{\text{OA}}(t_0) = \text{PF}_s(t_0) > 0$ and $\text{PF}_{\text{OPT}}(t_0) > 0$ for current time t_0 . As OA runs, $w_{\text{OA}}(t_0, t_1)$ is reduced at rate $\text{PF}_s(t_0)$. For $i > 0$, the value of $w_{\text{OA}}(i)$ remains unchanged. For the work done by OPT, we remark once more that OPT's speed profile does not necessarily align with breakpoints t_i . However, it is easy to verify that if at any point $t > t_0$ the speed $\text{PF}_{\text{OPT}}(t)$ increases, at least one new task will be released at time t . Therefore, assuming that no new tasks are released in the next dt units of time, we can assume $\text{PF}_{\text{OPT}}(t)$ to be a non-increasing step function over interval $[t_0, t_0 + dt)$. From this, we use that $\text{PF}_{\text{OPT}}(t_0)$ is an upper bound on the rate at which OPT reduces $w_{\text{OPT}}(t_0, t_1)$ throughout the next dt units of time. Therefore, for (22) to hold, it suffices to show that the following inequality holds:

$$\begin{aligned} & \text{PF}_s(t_0)^\alpha - \alpha^\alpha \text{PF}_{\text{OPT}}(t_0)^\alpha - \alpha \text{PF}_s(t_0)^{\alpha-1} \text{PF}_s(t_0) \\ & + \alpha^2 \text{PF}_s(t_0)^{\alpha-1} \text{PF}_{\text{OPT}}(t_0) \leq 0 \end{aligned}$$

Substituting $z = \frac{\text{PF}_s(t_0)}{\text{PF}_{\text{OPT}}(t_0)}$ results in

$$\text{PF}_{\text{OPT}}(t_0)^\alpha \left((1 - \alpha)z^\alpha + \alpha^2 z^{\alpha-1} - \alpha^\alpha \right) \leq 0,$$

where we note that in the working case, $\text{PF}_{\text{OPT}}(t_0) > 0$. Therefore, consider the polynomial

$$u(z) = (1 - \alpha)z^\alpha + \alpha^2 z^{\alpha-1} - \alpha^\alpha. \quad (23)$$

Evaluating this interval at the domain boundaries, we note that $\lim_{z \downarrow 0} u(z) = -\alpha^\alpha$ and $\lim_{z \uparrow \infty} u(z) = -\infty$ for $\alpha > 1$. For (22) to hold, it now suffices to show that the maximum of

(23) does not exceed zero. To this end, we differentiate the polynomial with respect to z , finding

$$\frac{du}{dz}(z) = (\alpha - \alpha^2)z^{\alpha-1} + (\alpha^3 - \alpha^2)z^{\alpha-2}.$$

Given that $z \neq 0$, this derivative assumes its unique zero in $z = \alpha$. Substituting this value into (23), we find the maximum value of $u(\alpha) = 0$, thereby proving (22) for the working case.

Lastly, we note that the arguments above also apply to the case where no new task arrives, but a task j is completed by OPT or OA at time t_0 . This is so since speed profiles $\text{PF}_{\text{OA}}(t)$ and $\text{PF}_{\text{OPT}}(t)$ are unaffected by the completion of j , allowing us to apply the working case arguments.

This concludes the proof of Lemma 10. \blacksquare

Theorem 12: OA is α^α -competitive for DSL.

Proof of Theorem 12: We first note that if we can upper bound the competitiveness by α^α , then this bound is tight. This follows directly from Lemma 3.2 in [13], where a DS instance is presented. A corresponding DSL instance given sufficiently large speed limits (e.g., speed limits $\ell_j = w_j = \left(\frac{1}{n-j}\right)^{\frac{1}{\alpha}}$), yields the same upper bound on the objective value and on the competitive ratio. For the details, we refer to [13].

As for the upper bound on the competitive ratio, we integrate (13) with regard to time to find that for any DSL instance I and corresponding OA schedule s_{OA} and optimal schedule s_{OPT} :

$$\int_t \text{PF}_{\text{OA}}(t)^\alpha + \int_t \frac{d\Phi(t)}{dt} \leq \alpha^\alpha \int_t \text{PF}_{\text{OPT}}(t)^\alpha \quad (24)$$

$$E(s_{\text{OA}}) + \Phi(\max_j d_j) - \Phi(\min_j r_j) \leq \alpha^\alpha E(s_{\text{OPT}}) \quad (25)$$

$$E(s_{\text{OA}}) \leq \alpha^\alpha E(s_{\text{OPT}}) \quad (26)$$

where all integrals in (24) are taken over the positive range $\mathbb{R}_{\geq 0}$. Furthermore, in (25) we use the definition of the objective function, the fundamental theorem of calculus, and Property 2 of Lemma 10. Finally, (26) follows from Property 1 of the same lemma, i.e., from $\Phi(\max_j d_j) = \Phi(\min_j r_j) = 0$. \blacksquare

D. Exact Scheduling Rules

As noted before, applying EDF may result in infeasible schedules for DSL instances (see Figure 3). This section takes this observation a step further, concluding that there exists no deterministic online scheduling rule that given any speed profile corresponding to a feasible schedule can guarantee to find such a schedule. In this, we assume that the scheduling rule only becomes aware of job j at its release time r_j , while the speed profile assumes implicit knowledge of all jobs released over the time horizon. Formally:

Theorem 13: Let I be a DSL instance, and let PF be a speed profile for which there exists a feasible schedule s for I such that $\text{PF}_s = \text{PF}$. There exists no deterministic online scheduling rule that reliably finds a feasible schedule s' for any such pair (I, PF) for which $\text{PF}_{s'} = \text{PF}$.

Proof of Theorem 13: We prove this by providing a speed profile and two DS instances corresponding to that profile, such that for any initial scheduling decision, one of the instances cannot be feasibly scheduled. A job set with five jobs is illustrated in Figure 10. We now consider two DSL instances that are

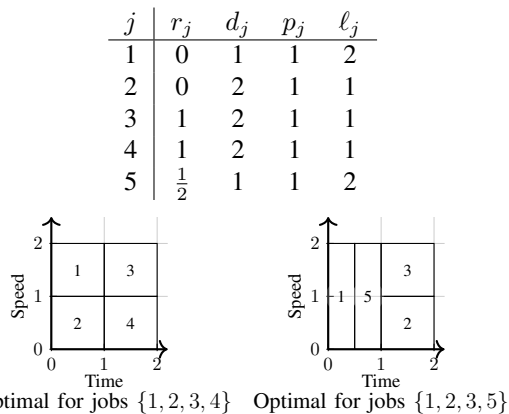


Fig. 10: Example instances for the proof that for DSL instances no online scheduling rule can reliably find a feasible schedule based on a speed profile.

subsets of those jobs. Here, the first instance I considers jobs $\mathcal{J} = \{1, 2, 3, 4\}$ and the second instance I' considers job set $\mathcal{J}' = \{1, 2, 3, 5\}$. Note that the optimal speed profile for both instances is constant with speed 2 throughout the time horizon $[0, 2]$. The respective optimal schedules are shown in the figure. Furthermore, at time $t = 0$, for both instances, only the first two jobs have been released.

Based on these two instances, we argue that for any scheduling decision made by an online algorithm at $t = 0$, we can choose an instance such that the resulting schedule cannot feasibly follow the speed profile. First, consider the case where at $t = 0$ the algorithm decides to only run Job 1. In that case, we reveal instance I . Limited by its speed limit, Job 2 cannot finish its processing before time $t = 1$ when Jobs 3 and 4 are released. Next, consider the case where on time interval $[0, \frac{1}{2}]$ Job 1 and Job 2 are processed at strictly positive speed for an $\epsilon > 0$ amount of time. If we now reveal instance I' , it is not possible anymore to follow the speed profile while completing both Jobs 1 and 5 before their respective deadlines. This illustrates that no deterministic online scheduling rule can reliably follow a given speed profile, even if there does exist a feasible schedule. \blacksquare

In particular, the result implies that there exists no 1-consistent learning augmented online scheduling algorithm for DSL that relies on predictions of the aggregated speed profile. Even if given the optimal speed profile, the proof above indicates that there exists no deterministic scheduling rule that can reliably find an optimal schedule.

V. NUMERICAL EXPERIMENTS

In this section, we relate the theory developed in the previous sections to the EV scheduling application. As theoretical competitive ratios assume worst case instances that may be very unrealistic to occur in practice, we compare the competitive ratios presented in Section IV with simulation results based on real-world data. We define the *empirical ratios* observed in the simulations in accordance with the definition of the competitive ratio in (10) to be $\frac{E(s^{\text{ALG}}(I))}{E(s^*(I))}$, where I is the considered instance, the numerator is the objective value of the considered (online) algorithm, and the denominator the objective value of the optimal solution.

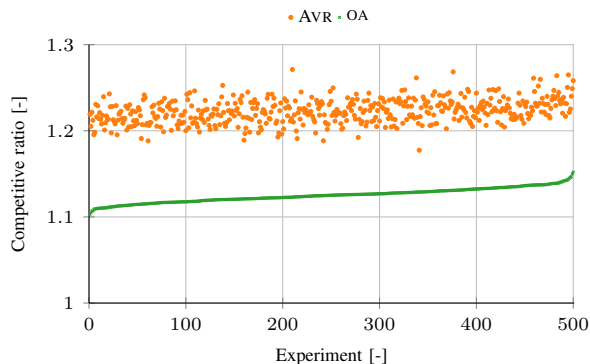


Fig. 11: Empirical ratios for AVR and OA for 500 instances of size 400. Their respective theoretical bounds are 8 and 4. Results sorted in increasing order based on their empirical ratios for OA.

The data was collected at an office parking lot in Utrecht, the Netherlands between September 1st 2022 and September 1st 2023, resulting in a total of 13694 charging sessions. A maximum of 113 charging sessions was recorded in a single day. Each recorded EV charging session is described by the EV’s arrival time, departure time and the total amount of energy charged. The charging stations at the parking lot are two-plug installations that support charging with at most 11 kW or 22 kW, depending on whether one or two EVs are plugged into the same charging station. In the experiments, we chose between these two values for the individual EV-specific maximum charging rates, depending on the average power required to charge the recorded amount of energy within the EV’s availability in the parking lot. Currently, there are around 250 chargers installed in the office parking lot, and this number is expected to increase to over 400 in the next few years.

For the numerical experiments, we randomly sampled 400 charging sessions and combined them into one instance. We solve this instance using FOCS, AVR and OA. As FOCS is an offline solver which results in an optimal solution (see Section III), we use its objective value for the calculation of the empirical ratios for online algorithms AVR and OA. We consider objective function (2) with $\alpha = 2$, and repeat the sampling and solving process 500 times, each time recording the objective value and power profile for the three algorithms.¹

The results are summarized in Figures 11 and 12. First, Figure 11 shows the empirical ratios for AVR (orange) and OA (green) for 500 randomly sampled instances. The instances have been sorted based on the empirical ratio for OA, resulting in the green dots forming an increasing sequence. Notably, this ordering has not translated to the empirical ratios of AVR, meaning that the ordering of two DSL instances based on the objective value for OA in general does not say anything about their objective values for AVR. For AVR the minimum and maximum empirical ratios recorded in the experiments were 1.18 and 1.27 respectively, as opposed to the theoretical bound $2^{\alpha-1}\alpha^\alpha = 8$. For OA the minimum and maximum empirical ratios were 1.10 and 1.15 respectively, as opposed to the theoretically tight competitive ratio $\alpha^\alpha = 4$. Note that the

¹The code used for the simulations is available under <https://github.com/lwinschermann/FlowbasedOfflineChargingScheduler> (commit 7506297).

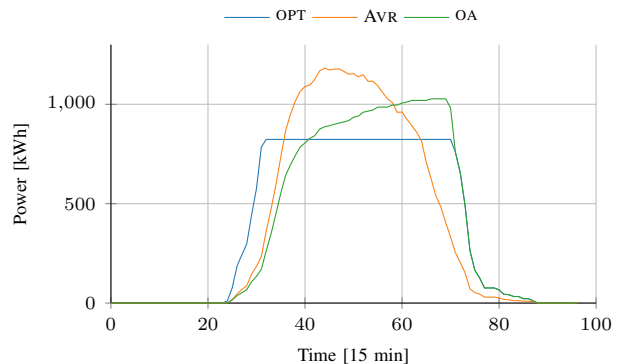


Fig. 12: Aggregated speed profiles for FOCS, OA and AVR for one sampled instance based on real-world data.

maximum empirical ratio for OA is smaller than the minimum for AVR. That implies that in terms of objective value, OA dominates AVR.

For a randomly chosen experiment, Figure 12 shows the three power profiles resulting from FOCS (blue), AVR (orange) and OA (green). The speed profile of AVR is more impacted by the high simultaneity of arrivals and great variance of departure times in this particular office building [22]. The effect is graphically reflected by the slightly left-leaning form of the curve. Its relative smoothness can be attributed to the long dwell times and simultaneity in office parking lots. OA, on the other hand, shifts a lot of the work to the end of the time horizon, as it is oblivious to each subsequent new arrival. From a user perspective, having a gradual charging process over the day invokes less anxiety and mistrust as opposed to charging later in the day. Furthermore, the AVR solution is more robust to early departure by individual EVs. This last observation falls outside of the DSL problem statement, but becomes relevant when considering e.g., charging guarantees as deterministic input to the optimization.

VI. CONCLUSION

In this work, we consider an EV scheduling problem with as objective to minimize an increasing, convex and differentiable function of the aggregated power profile. To this end, we relate EV charging to speed scaling with job-specific speed limits and derive sufficient and necessary optimality conditions. Furthermore, we present an offline algorithm that determines an optimal schedule in $\mathcal{O}(n^2\mu)$ time where μ is the run time of any efficient maximum flow algorithm. We argue that this run time can further be reduced by exploiting the underlying problem structure of the EV scheduling problem. Lastly, we provide a mathematical proof of the optimality of the algorithm.

Next to the offline algorithm, we analyze two online algorithms and their respective competitive ratios for a class of objective functions depending on a parameter α . Average Rate is shown to be $2^{\alpha-1}\alpha^\alpha$ competitive, and Optimal Available has a tight competitive ratio α^α where α is a parameter in the considered objective function. These competitive ratios match those for the classical speed scaling model that has no job-specific speed limits. We put those results into perspective

by comparing them to empirical ratios based on real-world EV charging data.

Future work may investigate additional problem constraints such as global power limits. Furthermore, numerical experiments are of interest, especially their integration with control strategies such as model predictive control or fill-level algorithms. Lastly, given that optimal schedules are not necessarily unique, scheduling rules resulting in a robust output should be explored.

REFERENCES

- [1] J. W. Eising, T. van Onna, and F. Alkemade, "Towards smart grids: Identifying the risks that arise from the integration of energy and transport supply chains," *Applied Energy*, vol. 123, pp. 448–455, 2014. [Online]. Available: <https://www.sciencedirect.com/science/article/pii/S0306261913010167>
- [2] K. Turitsyn, N. Sinitsyn, S. Backhaus, and M. Chertkov, "Robust broadcast-communication control of electric vehicle charging," in *2010 First IEEE International Conference on Smart Grid Communications*, 2010, pp. 203–207.
- [3] G. Vecchio and L. Tricarico, "'may the force move you': Roles and actors of information sharing devices in urban mobility," *Cities*, vol. 88, pp. 261–268, 2019. [Online]. Available: <https://www.sciencedirect.com/science/article/pii/S0264275118307522>
- [4] G. Van Krieking, C. De Cauwer, N. Sapountzoglou, T. Coosemans, and M. Messagie, "Peak shaving and cost minimization using model predictive control for uni- and bi-directional charging of electric vehicles," *Energy Reports*, vol. 7, pp. 8760–8771, 2021.
- [5] M. A. S. T. Ireshika and P. Kepplinger, "Uncertainties in model predictive control for decentralized autonomous demand side management of electric vehicles," *Journal of Energy Storage*, vol. 83, p. 110194, 2024. [Online]. Available: <https://www.sciencedirect.com/science/article/pii/S2352152X23035934>
- [6] L. Winschermann, G. Hoogsteen, and J. Hurink, "Integrating guarantees and veto-buttons into the charging of electric vehicles at office buildings," in *2023 IEEE PES Innovative Smart Grid Technologies Europe (ISGT EUROPE)*, 2023, pp. 1–5.
- [7] M. H. H. Schoot Uiterkamp, M. E. T. Gerards, and J. L. Hurink, "Fill-level prediction in online valley-filling algorithms for electric vehicle charging," in *2018 IEEE PES Innovative Smart Grid Technologies Conference Europe (ISGT-Europe)*, 2018, pp. 1–6.
- [8] F. Yao, A. Demers, and S. Shenker, "A scheduling model for reduced CPU energy," in *Annual Symposium on Foundations of Computer Science*. IEEE Computer Society, 1995, pp. 374–382.
- [9] V. Vizing, L. Komzakova, and A. Tarchenko, "An algorithm for selecting the execution intensity of jobs in a schedule," *Cybernetics*, vol. 17, pp. 646–649, 1982, english. Russian original in *Kibernetika* 1981 no. 5, 71–74.
- [10] A. Antoniadis, P. Kling, S. Ott, and S. Riechers, "Continuous speed scaling with variability: A simple and direct approach," *Theoretical Computer Science*, vol. 678, pp. 1–13, 2017.
- [11] A. Shioura, N. Shakhlevich, and V. Strusevich, "Machine speed scaling by adapting methods for convex optimization with submodular constraints," *Inform Journal on Computing*, vol. 29, pp. 724–736, 2017.
- [12] Z. Zhang, L. F., and H. Aydin, "Optimal speed scaling algorithms under speed change constraints," in *2011 IEEE International Conference on High Performance Computing and Communications*, 2011, pp. 202–210.
- [13] N. Bansal, T. Kimbrel, and K. Pruhs, "Speed scaling to manage energy and temperature," *J. ACM*, vol. 54, no. 1, mar 2007.
- [14] J. L. W. V. Jensen, "Sur les fonctions convexes et les inégalités entre les valeurs moyennes," *Acta Mathematica*, vol. 30, no. none, pp. 175 – 193, 1906. [Online]. Available: <https://doi.org/10.1007/BF02418571>
- [15] S. Boyd and L. Vandenberghe, *Convex Optimization*. Cambridge University Press, 2004.
- [16] J. Edmonds and R. M. Karp, "Theoretical improvements in algorithmic efficiency for network flow problems," *J. ACM*, vol. 19, no. 2, p. 248–264, apr 1972.
- [17] L. R. Ford and D. R. Fulkerson, "Maximal flow through a network," *Canadian Journal of Mathematics*, vol. 8, p. 399–404, 1956.
- [18] Y. Dinitz, "Algorithm for solution of a problem of maximum flow in networks with power estimation," *Soviet Math. Dokl.*, vol. 11, pp. 1277–1280, 01 1970.
- [19] A. Karzanov, "Determining the maximal flow in a network by the method of preflows," *Doklady Mathematics*, vol. 15, p. 434–437, 02 1974.
- [20] A. V. Goldberg and R. E. Tarjan, "A new approach to the maximum-flow problem," *J. ACM*, vol. 35, no. 4, p. 921–940, oct 1988.
- [21] N. Bansal, K. Pruhs, and C. Stein, "Speed scaling for weighted flow time," *SIAM Journal on Computing*, vol. 39, no. 4, pp. 1294–1308, 2010. [Online]. Available: <https://doi.org/10.1137/08072125X>
- [22] L. Winschermann, N. Bañol Arias, G. Hoogsteen, and J. Hurink, "Assessing the value of information for electric vehicle charging strategies at office buildings," *Renewable and Sustainable Energy Reviews*, vol. 185, p. 113600, 2023. [Online]. Available: <https://www.sciencedirect.com/science/article/pii/S1364032123004574>